RESEARCH ARTICLE

Electrochemical Studies of Carbonated Hydroxyapatite/CHS Nanocomposite†

C. P. DHANALAKSHMI[a], L. VIJAYALAKSHMI[b],
R. SURESH[a], K. GIRIBABU[a] and V. NARAYANAN[a*]

[a]Department of Inorganic Chemistry, University of Madras, Guindy Maraimalai Campus, Chennai-600025, Tamilnadu, India
[b]Vidhya Sagar Women's College, Chengalpattu, Kancheepuram, Chennai-603211, Tamilnadu, India
vnnara@yahoo.co.in

Abstract: Carbonated hydroxyapatite /CHS nanocomposites of varying composition for biomaterial applications have been synthesized. The Carbonated hydroxyapatite /CHS nanocomposite materials were characterized by XRD, FTIR, FESEM, EDAX, HRTEM and XPS. Carbonated hydroxyapatite (CHAp) nanorod embedded composite was prepared using chitosan (CHS) as a matrix with different weight percentages (wt %). The results indicated that the size and crystallinity of CHAp nano particles decreases with increase in CHS concentration in the composite. FESEM confirms the presence of CHAp nanorod crystals in CHS matrix. Cyclic voltammograms (CVs) were recorded to evaluate the electrocatalytic behaviors of the modified electrode towards the oxidation of 4-NP in the potential range of 0 to +1.0 V. A glassy carbon electrode was modified with carbonated hydroxyapatite nanopowder (CHAp-NP) and characterized in terms of electrochemical oxidation of 4-nitrophenol (4-NP) via cyclic voltammetry. The catalytic reaction facilitates electron transfer between 4-NP and the modified electrode, as a result the electrochemical oxidation of 4-NP becomes easier. The reason for this is that the CHAp-CHS 80 can act as a promoter to increase the rate of electron transfer, lower the overpotential of 4-NP at the bare electrode, and the anodic peak shifts less positive potential. Thus, it is clear that CHAp-CHS 80 modified GCE can be successfully used for the determination of organic pollutant.

Keywords: Carbonated hydroxyapatite, Electrochemical oxidation, Nanocrystalline, Chitosan

Introduction

A critical challenge in the design of these hybrid inorganic-organic systems is a control of the mixing between the two dissimilar phases. A composite material is a macroscopic combination of two or more distinct materials, having a recognizable interface between them. Composites are used not only for their structural properties, but also for electrical, thermal, tribological and environmental applications. Modern composite materials are usually optimized to achieve a particular balance of properties for a given range of applications.

†Presented to the National Conference on Chemistry Solutions at SRM University, India

4-NP is widely used as intermediates in the production of pharmaceuticals, pesticides and dyestuffs, such as parathion insecticide which can also reversely hydrolyze to form 4-NP. In addition, 4-NP can also be used as leather fungicide and acid-base indicator. Therefore, 4-NP will be inevitably released into environment to cause pollution in the process of fabrication and application. Based on the above description, it is important to develop simple and reliable method for determination of trace amounts of 4-NP in environments[1,2]. Up to now, various techniques have been investigated to determine 4-NP, such as spectrophotometry, fluorescence, high-performance liquid chromatography[3], liquid chromatography with electrochemical detection, capillary zone electrophoresis[4], fiber optode[5] and electrochemical method[6]. Among them, electrochemical methods have received considerable attention because of the advantage of fast response, cheap instrument, low cost, simple operation, timesaving, high sensitivity and selectivity, real-time detection in in-situ condition. However, until now, many electrochemical determination techniques mainly focus on utilizing the reduction of nitryl in 4-NP, not the oxidation of hydroxide radical. Thus, the determination would be interfered by the oxygen molecule dissolved in solvent. In order to eliminate it, purging nitrogen for a certain time was employed. But this will make the determination more complicated and time-consuming. Moreover, the reduction of nitryl is more complicated than the oxidation of hydroxide radical. Therefore, electrochemical determination of 4-NP using the oxidation signal should be an appropriate alternative. Nevertheless, the use of bare electrode has revealed the drawback of weak electrochemical response and low sensitivity. Consequently, chemically modified electrodes (CMEs) have been widely investigated with various modification materials, especially nanophase materials, such as MWCNT[7], SWCNT[8], gold nanoparticles[9], TiO_2,[10] zeolite[11], sodium montmorillonite[12] and HAp[13,14]. Among them, nano HAp has advantages of abundant in nature, cheap, readily available and stable in water and nontoxicity. Due to the high surface area and strong adsorption ability, a film of silica/HRP-HAp has been deposited on GCE surface to investigate the direct electron transfer of immobilized HRP and H_2O_2 determination[15]. El Mohammedi *et al*. have evaluated the analytical performance of nano HAp-CPE for the detection of trace lead (II), paraquat and 4-NP. They found that HAp can effectively improve the electrochemical response due to its excellent adsorption property[16,17]. So, nano HAp should be a suitable electrode modified material for pollution determination.

The aim of the present work is to develop a simple, reliable and sensitive electrochemical method for the determination of 4-NP(4-nitrophenol) based on the unusual properties of polymer composites of nano CHAp-CHS -NP modified electrode. The modified electrode showed good electrochemical oxidation to 4-NP with an increase of the oxidation peak current. The electrocatalytic determination of nitrophenols were carried out using the polymer nanocomposite modified electrodes and found to be good sensors for the detection of nitro organic compounds.

Experimental

The raw materials required to start the processing of the composite were: analytical grade calcium hydroxide $(Ca(NO_3)_2)$, $(NH_4)_2HPO_4$ and $(NH_4)_2CO_3$ obtained from Merck (India) and PEG (MW 6000) purchased from Loba (India). Doubly distilled water was used as the solvent.

Methods

Synthesis of nano CHAp

The nano CHAp was synthesized by following a modified wet chemical method. $Ca(NO_3)_2$ and PEG were dissolved in 50 mL distilled water to form a $Ca(NO_3)_2$ solution with a

PEG:Ca^{2+} weight ratio of 4:1. $(NH_4)_2HPO_4$ and $(NH_4)_2CO_3$ were first dissolved in 50 mL distilled water to form a clear 0.10 M phosphate solution with an initial molar ratio of CO_3/PO_4 of 1:1 and then added drop wise to the polymer-$Ca(NO_3)_2$ solution with an initial Ca/P molar ratio of 1.60; the precipitation reaction was maintained at 5 ^{o}C under vigorous stirring for 30 min. The powder sample of CHAp was obtained after heat treating the precipitate at 800 ^{o}C for 3 h in a furnace filled with air.

Synthesis of CHAp-CHS nanocomposites

The CHAp-CHS nanocomposite was synthesized by freeze gelation method. Water was used as the solvent to prepare polymer solution. CHS was dissolved by using magnetic stirrer for 3h and the polymer solution was left overnight in room temperature to remove the air bubbles trapped in the viscous solution. Then suitable amount of CHAp was dispersed in deionised water by 30 min ultrasonication. Ultrasonication was necessary to avoid agglomeration of ceramic powder and to achieve proper dispersion. CHAp in water was mixed with polymer solution under agitation. The homogeneously mixed solution is immediately taken to deep freeze at –18 ^{o}C. After 48 h freezing the samples were freeze dried. The CHAp-CHS nano composites were coded as CHAp-CHS 20 to CHAp-CHS 80 where number denotes the wt% of CHS.

Physical-chemical characterization

The prepared samples were studied by Fourier Transform Infrared Spectroscopy (FTIR) using a Schimadzu FT-IR 300 series instrument (Shimadzu Scientific Instruments, USA). The FTIR spectra were obtained over the region 450–4000 cm^{-1} in pellet form for 1 mg powder samples mixed with 200 mg spectroscopic grade KBr (). Spectra were recorded at 4 cm^{-1} resolution averaging 80 scans. The structure of the samples were analyzed by X-Ray Diffraction (XRD) using a Rich Siefert 3000 diffractometer (Seifert, Germany) with Cu-Kα_1 radiation (λ = 1.5418 Å). In this work a JEOL FX 2000 Transmission Electron Microscope and FEI Teccani F30 High Resolution Transmission Electron Microscope were used to study the morphology of the nanoparticles with a resolution of 5 Å – 10 Å. The powder samples were dispersed in Gatan G1 epoxy resin and dried at 353 K to get a hard and thick disc. Then thick discs were sliced to small pieces and mechanically polished to ~ 0.15 μm.

Results and Discussion
Characterization of CHAp-CHS nanocomposites
FT-IR analysis

The FT-IR spectra of pure nano CHAp and CHAp-CHS nanocomposites are shown in Figure 1 The ν_2 phosphate stretching mode is appeared at 527 cm^{-1} corresponds to PO_4^{3-} group in CHAp. The bands appeared at 1073-1114 cm^{-1} and 527-585 cm^{-1} corresponds to different modes of the PO_4^{3-} group in carbonated hydroxyapatite. The observed bands at 602 cm^{-1} corresponds to O-P-O bending and ν_1 symmetric P-O stretching modes. The ν_1 symmetric stretching mode of phosphate group is observed at 955-962 cm^{-1}. The observed bands at 1384-1466 and 805-872 cm^{-1} are assigned to carbonate ions. The peak appeared at 1633-1649 cm^{-1} (amide I) with a minor shoulder at 1564 cm^{-1} (amide II) are attributed to acetylated amino and confirms that sample is not fully deacetylated. The peak at 1384 cm^{-1} was assigned to C-O stretching of primary alcoholic group (-CH_2OH) and the peak at 900 cm^{-1} is attributed to the C-O stretching. The bands at 1550–1700 cm^{-1} are attributable to mode super position of the hydroxyapatite OH^{-} group and the CHS amide I and amide II groups[17-20]. A broad band appears from 3433-3436 and 2919 cm^{-1} corresponding to the broad –OH stretching bands between 3100-3450 cm^{-1} and the aliphatic C-H stretching bands between 2918-2925 cm^{-1}.
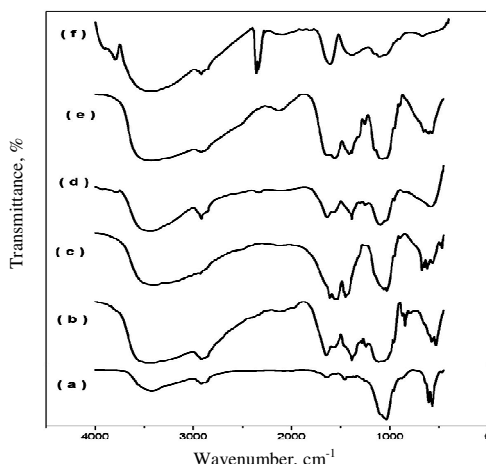
Figure 1. FTIR Spectra of (a) nano CHAp, (b) CHAp-CHS 20, (c) CHAp-CHS 40,
(d) CHAp-CHS 60, (e) CHAp-CHS 80 and (f) CHS

X-ray diffraction analysis

The XRD patterns of nano CHAp and CHAp-CHS nanocomposites were taken. The patterns indicate the presence of amorphous CHAp. The broad peaks reveal that the particles sizes are very small in the range of 33 to 34 nm. The reflection planes corresponding to the characteristic XRD spectral peaks of pure nano CHAp and CHAp-CHS nanocomposites are shown in Figure 2. The observed diffraction peaks are identified by standard JCPDS file (File No. 35-0180) and are assigned as crystalline CHAp. The XRD patterns show diffraction peaks with line broadening and high intensities, which confirms the nano size with crystalline nature. The crystallite size of the pure nano CHAp and CHAp-CHS nanocomposite is calculated by using Scherrer's formula. Figure 2 reveals that the crystallite size of nano CHAp decreases with increase in the composition of CHS.
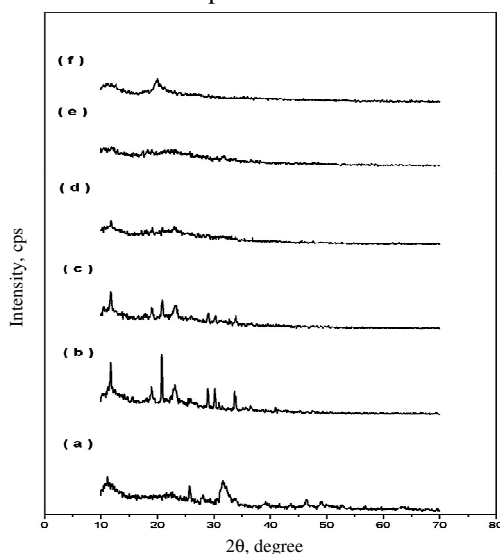

Figure 2. XRD Pattern of (a) nano CHAp, (b) CHAp-CHS 20, (c) CHAp-CHS 40,
(d) CHAp-CHS 60, (e) CHAp-CHS 80 and (f) CHS

FESEM and EDAX analysis

FESEM images of pure nano CHAp and different weight percentages of CHS compositions are illustrated in Figure 3. The FESEM picture shows that particles exhibit nanorod morphology. The particle size of pure nano CHAp is 25-70 nm. In case of composites, when the composition of CHS is added to CHAp, the rod-like morphology starts to disappear. The increase in the CHS compositions *i.e*., 20, 40, 60 wt. % leads to a corresponding change from rod-like to an irregular morphology. Further, it is evident that the particle size decreases with increase in CHS composition. The elemental analysis (EDAX) of CHAp-CHS 40 nanocomposite is illustrated in Figure 3a. Mineral composition (calcium phosphate: Ca, O, P) and organic content © present in the nanocomposite CHAP-CHS is tested.
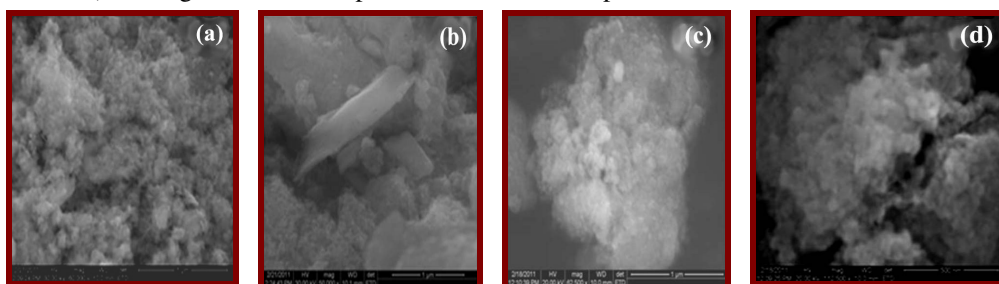

Figure 3. FE-SEM images of (a) nano CHAp, (b) CHAp-CHS 20, (c) CHAp-CHS 40 and (d) CHAp-CHS 60
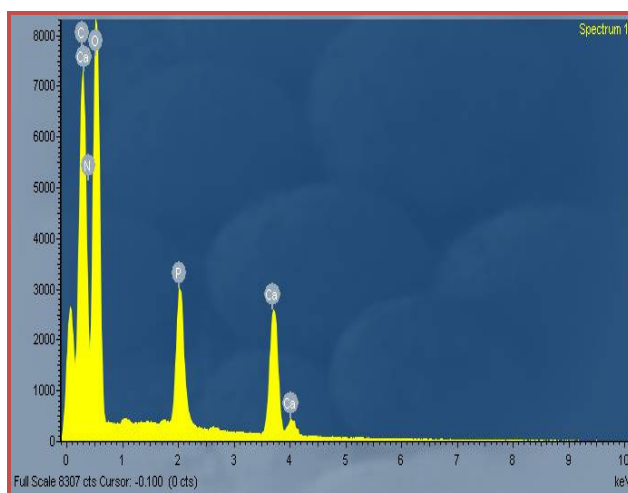

Figure 3a. EDAX spectrum of CHAp-CHS 40 nanocomposite

HR TEM analysis

Figure 4 shows the HRTEM photograph of CHAp-CHS 20 nanocomposite powder. The CHAp-CHS 20 nanocomposite particles shown in Figure 4 are in nanometer scale. This core/shell nanoparticles are finding widespread application. There is a class of core/shell nanoparticle that has its entire constituent in the nanometer range. Core/shell nanoparticles are nano structures that have core made of a material coated with another material. They are in the size range of 8 nm to 40 nm. Also, composite structures with these core/shell particles embedded in a matrix material are in use. Taking into consideration the size of the nanoparticles, the shell material can

be chosen such that the agglomeration of particle can be prevented. This implies that the mono dispersity of the particle can be improved. The core/shell structure enhances the thermal and chemical stability of the nanoparticles, improves solubility, makes them less cytotoxic and allows conjugation of other molecules to these particles.

CHAp-CHS 20 nanocomposite particles were a bit thicker (5-40 nm) and longer with clear contour. In addition the particles showed less agglomeration. In addition the selected area electron diffraction (SAED, in Figure 4a) of the precipitates shows with diffraction ring of patterns, which implies that the precipitates are crystalline in nature, which is agreed by XRD results.
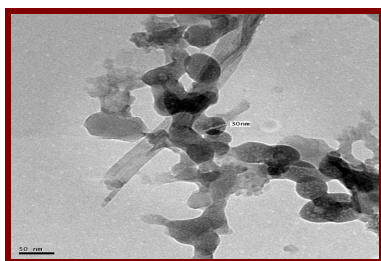

Figure 4. HRTEM image of CHAp-CHS 20 nanocomposite

Figure 4a. SAED image of CHAp-CHS 20 nanocomposite

X-ray photoelectron spectroscopy (XPS)

A representative survey spectrum for HAp-CHS 20 nanocomposite powder obtained at 30 °C is presented in Figure 5 together with the expected positions of the main lines (Ca 2p at 347.10 eV, O 1s at 531 eV and P 2p at 133.8 eV respectively. For XPS analysis the binding energies were calibrated with reference to C 1s at 285 eV. The Ca(2p) signal is composed of two lines Ca 2p1/2 (350.67 eV) dedicated to calcium apatite and Ca 2p 3/2(347.13 eV) relate to a simple Ca-O bond. As a general observation the ratio Ca/P is nearly stoichiometric.
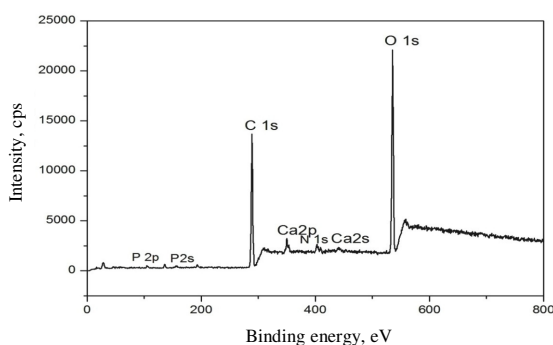

Figure 5. X-Ray photoelectron (survey) spectrum of CHAp-CHS 20 nanocomposite

Electrochemical studies

Detection of 4-nitrophenol

Cyclic voltammograms (CVs) were recorded to evaluate the electrocatalytic behaviors of the modified electrode towards the oxidation of 4-NP (4-nitrophenol) in the potential range of 0 to +1.0 V. Figure 6 depicts the CV's of bare, nano CHAp, nanocomposites of CHAp-CHS 20, CHAp-CHS 40, CHAp-CHS 60 and CHAp-CHS 80 modified GCE respectively in the presence of 0.5 mM 4-NP in 0.1 M PBS(Phosphate Buffer solution). The CV of 4-NP (Figure 1)

(Figure 6) at bare GCE shows a very broad peak at about +0.92 V. The 4-NP voltammogram obtained at CHAp modified GCE showed an oxidation potential at +0.75 V (Figure 6). However, the 4-NP voltammogram obtained for nanocomposites of CHAp-CHS 20, CHAp-CHS 40, CHAp-CHS 60 and CHAp-CHS 80 modified GCE showed well defined oxidation wave of 4-NP with cathodic shift in potential and variation of the oxidation peak current correspond to the bare and nano CHAp modified GCE, indicating the electrocatalytic ability of the modified GCE.[21-25] From the Figure 6, it can be seen that the oxidation potential and current response of 4-NP varied with the amount of the added CHS. Especially CHAp-CHS 80 modified GCE showed higher oxidation peak current with lower oxidation potential at +0.73 V. The overpotential had thus decreased by 0.19 V indicating the strong electrocatalytic effect of CHAp-CHS 80 modified layer.
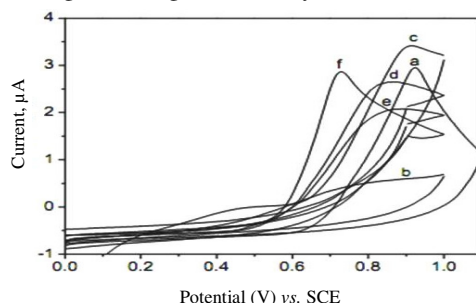

Figure 6. CV of 0.5 mM 4-NP at (a) bare, (b) nano CHAp, (c) CHAp CHS 20, (d) CHAp-CHS 40, (e) CHAp-CHS 60 and (f) CHAp-CHS 80 modified GCE in the scan rate of 10 mV s^{-1}

The above results indicate that catalytic reaction occurred between the CHAp-CHS 80 with 4-NP. The catalytic reaction facilitates electron transfer between NPs and the modified electrode, as a result the electrochemical oxidation of NPs becomes easier. The reason for this is that the CHAp-CHS 80 can act as a promoter to increase the rate of electron transfer, lower the overpotential of NPs at the bare electrode and the anodic peak shifts less positive potential. Thus, it is clear that CHAp-CHS 80 modified GCE can be successfully used for the determination of organic pollutant.

Conclusion

The conclusions drawn from this work are the FTIR and XRD analysis of the CHAp-CHS nano composites showed that both the components exist in the composite. The XRD pattern shows diffraction peaks with line broadening and high intensities, which confirms the nanosize with crystalline nature. HRTEM photograph of CHAp-CHS nanocomposite showed that the particles are in nanometer scale (10-40 nm). In addition, the particles showed less agglomeration. The selected area electron diffraction (SAED) studies showed that diffraction ring of patterns which implies that the ceramic particles are crystalline in nature, which is also proved by XRD results. The CHAp-CHS nanocomposites modified GCE showed good electrocatalytic activity towards the detection of 4-NP. The oxidation peak potentials for the nitrophenols are shifted to lower anodic region for the modified electrodes compared to bare GCE. This study will be useful for the detection of environmental organic pollutants and also traces of explosives.

References

1.   Niazi A and Yazdanipour A A, *J Hazard Mater.,* 2007, **146(1-2),** 421-427.
2.   Nistor C, Oubina A, Marco M P, Barceló D and Emnéus J, *Anal Chim Acta,* 2001, **426**, 185-195.

3.   Thompson M J, Ballinger L N, Cross S E and Roberts M S, *J Chromatogr B,* 1996, **677**, 117-122.
4.   Galeano-Diaz T, Guiberteau-Cabanillas A, Mora-Diez N, Parrilla-Vazquez P and Salinas-Lopez F, *J Agric Food Chem*., 2000, **48(10)**, 4508-4513.
5.   Guo X, Wang Z and Zhou S, *Talanta*. 2004, **64**, 135-139.
6.   Yang X, Shen G and Yu R, *Microchim Acta*, 2001, **136**, 73.
7.   Huang W, Yang C and Zhang de S, *Anal Bioanal Chem.*, **375**, 703.
8.   Yang C H, *Microchim Acta,* 2004, **148**, 87-92.
9.   Liu Z, Du J, Qiu C, Huang L, Ma H, Shen D and Ding Y, *Electrochem Commun* 2009, **11,** 1365
10.   Kafi A K M and Chen A, *Talanta*, 2009, **79(1),** 97-102.
11.   Del Mar Cordero-Rando M, Barea-Zamora M, Barberá-Salvador J M, Naranjo-Rodríguez I, Muñoz-Leyva J A and Hidalgo-Hidalgo de Cisneros J L, *Microchim Acta*, 1999, **132,** 7.
12.   Hu S, Xu C, Wang G and Cui D, *Talanta,* 2001, **54(1),** 115-123.
13.   El Mhammedi M A, Achak M, Bakasse M and Chtaini A, *J Hazard Mater*., 2009, **163(1)**, 323-328.
14.   Lin K, Pan J, Chen Y, Cheng R and Xu X, *J Hazard Mater*., 2009, **161(1),** 231-240.
15.   Wang B, Zhang J J, Pan Z Y, Tao X Q and Wang H S, *Biosens Bioelectron*., 2009, **24(5)**, 1141-1145.
16.   El Mhammedi M A, Achak M and Chtaini A, *J Hazard Mater*., 2009, **161,** 55-61.
17.   Kong L, Gao Y, Lu G, Gong Y, Zhao N and Zhang X, *Eur Polym J*., 2006, **42**, 3171-3179.
18.   El Mhammedi M A, Bakasse M and Chtaini A, *Electroanalysis*, 2007, **19(16),** 1727-1733.
19.   Killoy W J, *Int Dent J.,* 1998, **48(3),** 305-315.
20.   Raynaud S, Champion E and Bernache-Assollant D, *Biomaterials,* 2002, **23,** 1073-1080.
21.   Fischer J, Vanourkova L, Danhel A, Vyskocil V, Cizek K, Barek J, Peckova K, Yosypchuk B and Navratil T, *Int J Electrochem Sci.,* 2007, **2,** 226-234.
22.   Choudhury A, Bhowmick A K and Ong C, *Polymer*, 2009, **50**, 201-210.
23.   Huanshun Yin, Yunlei Zhou, Shiyun Ai, Xianggang Liu, Lusheng Zhu and Linan Lu. *Microchim Acta*, 2010, **169(1-2),** 87-92.
24.   Dhanalakshmi C P, Vijayalakshmi L and Narayanan V, *Int J Nano Mater Sci*., 2012, **1(2),** 81-96.
25.   Niaz A, Fischer J, Barek J and Yosypchuk B, *Electroanalysis*, 2009, **21,** 1786-1791.